NEUROSCIENCE
RESEARCH ARTICLE

Andrey Tsoy et al. / Neuroscience 408 (2019) 46–57

The Effects of Mobile Phone Radiofrequency Electromagnetic Fields on β-Amyloid-Induced Oxidative Stress in Human and Rat Primary Astrocytes

Andrey Tsoy,[a] Timur Saliev,[a,b] Elvira Abzhanova,[a] Anel Turgambayeva,[a] Aiym Kaiyrlykyzy,[a] Mars Akishev,[a] Samat Saparbayev,[c] Bauyrzhan Umbayev[a] and Sholpan Askarova[a,*]

[a]*National Laboratory Astana, Nazarbayev University, 53 Kabanbay batyr Ave., Astana, 010000, Kazakhstan*

[b]*S.D. Asfendiyarov Kazakh National Medical University, Tole Bi Street 94, Almaty, 050000, Kazakhstan*

[c]*National Scientific Medical Center, 42 Abylai Khan Ave, Astana, 010000, Kazakhstan, 010009*

Abstract—Amyloid beta peptide (Aβ) is implicated in the development of pathological reactions associated with Alzheimer's disease (AD), such as oxidative stress, neuro-inflammation and death of brain cells. Current pharmacological approaches to treat AD are not able to control the deposition of Aβ and suppression of Aβ-induced cellular response. There is a growing body of evidence that exposure to radiofrequency electromagnetic field (RF-EMF) causes a decrease of beta-amyloid deposition in the brains and provides cognitive benefits to Alzheimer's Tg mice. Herein, we investigated the effects of mobile phone radiofrequency EMF of 918 MHz on reactive oxygen species (ROS) formation, mitochondrial membrane potential (MMP), activity of NADPH-oxidase, and phosphorylation of p38MAPK and ERK1/2 kinases in human and rat primary astrocytes in the presence of $A\beta_{42}$ and H_2O_2. Our data demonstrate that EMF is able to reduce $A\beta_{42}$- and H_2O_2-induced cellular ROS, abrogate Aβ-induced production of mitochondrial ROS and the co-localization between the cytosolic (p47-phox) and membrane (gp91-phox) subunits of NADPH oxidase, while increasing MMP, and inhibiting H_2O_2–induced phosphorylation of p38MAPK and ERK1/2 in primary astrocytes. Yet, EMF was not able to modulate alterations in the phosphorylation state of the MAPKs triggered by $A\beta_{42}$. Our findings provide an insight into the mechanisms of cellular and molecular responses of astrocytes on RF-EMF exposure and indicate the therapeutic potential of RF-EMF for the treatment of Alzheimer's disease. **© 2019 IBRO. Published by Elsevier Ltd. All rights reserved.**

Key words: Alzheimer's disease, astrocytes, β-amyloid, electromagnetic field, oxidative stress.

INTRODUCTION

Alzheimer's disease (AD) is an incurable chronic neurodegenerative disorder characterized by dramatic loss of memory and progressive cognitive decline. AD incidence increases with age and is shown to affect approximately 10% of people aged 65–75 and 32% of the elderly aged 80 and above (Prince et al., **2016**; Anon, **2018**). It is believed that the pathophysiology of AD is driven by accumulation of amyloid plaques, consisting of an insoluble form of amyloid beta peptide (Aβ) in the brain leading to neuro-inflammation, oxidative stress, mitochondrial dysfunction, dysregulation of enzyme systems (phosphatases, kinases, and proteases) and neuronal death. However, current clinical trials directed at lowering Aβ levels and decreasing levels of toxic Aβ aggregates in the brain have failed and a number of novel approaches are still in consideration and development (Lukiw, **2012**). Moreover, in recent years it has become clear that it is not the fibrillar β-amyloid but the soluble oligomers of the peptide that are responsible for the neuronal death and disruption of cognitive function. Although precise mechanism of Aβ oligomers neurotoxic effects remains unclear, numerous in vivo and in vitro studies have demonstrated that Aβ oligomers initiate oxidative stress and neuro inflammation, induce synapse deterioration and loss, affect calcium homeostasis and long-term potentiation, cause neurodegeneration by forming large, voltage independent, and nonselective ion channels (Cline et al., **2018**).

As an alternative to pharmacological approach towards treatment of Alzheimer's disease, various biophysical methods such as ultrasound (Leinenga and Gotz, **2015**), laser (Hanczyc et al., **2013**; Mohammad et al., **2015**) and electromagnetic fields (Arendash et al., **2010**) have been proposed in the recent decades. Despite a high therapeutic potential demonstrated in experimental studies, those methods bear

*Corresponding author. Tel.: + 7 7172 70 65 14.
E-mail address: shaskarova@nu.edu.kz (Sholpan Askarova).

Abbreviations: Aβ, Amyloid beta peptide; AD, Alzheimer's disease; RF-EMF, Radiofrequency electromagnetic fields; ROS, Reactive oxygen species; EMF, Electromagnetic field; RF, Radiofrequency; CM-H2DCFDA, Chloromethyl derivative of 2′,7′-dichlorodihydrofluorescein diacetate; NOX, NADPH oxidase; MAPK, Mitogen-activated protein kinase; ERK 1/2, Extracellular signal-regulated kinases 1 and 2; HFIP, 1,1,1,3,3,3 hexafluoro-2-propanol; SAR, Specific absorption rate.

https://doi.org/10.1016/j.neuroscience.2019.03.058
0306-4522/© 2019 IBRO. Published by Elsevier Ltd. All rights reserved.

some intrinsic limitations. For instance, application of ultrasound and laser requires a close contact with the skull and affected brain tissues. Moreover, treatment by high intensity focused ultrasound has been associated with serious problems such as heating of surrounding tissues that can cause discomfort and pain (Kennedy, **2005**; Li et al., **2009**). In comparison with other biophysical methods, application of non-ionizing electromagnetic fields (EMFs) provides an exceptional depth of tissue penetration and complete non-invasiveness.

All bio-medical applications of EMFs could be roughly subdivided into two categories: utilizing thermal and non-thermal EMF-induced effects. Harnessing EMF thermal effect has been proposed as an alternative to traditional surgical resection for tumor ablation (Manthe et al., **2010**). This approach predominantly relies on the use of radiofrequency (RF) and microwave ablation. On the other hand, there is evidence that the non-thermal aspect of RF-EMF can be employed for the treatment of some neurological dysfunctions. Arendash et al. experimentally demonstrated that prolonged exposure of brain to EMF caused a decrease of β-amyloid deposition in brain (Arendash et al., **2012**). In a previous study, Arendash et al. exposed old AD transgenic mice to RF-EMF with characteristics similar to mobile phone radiation (GSM, pulsed modulated signal, 918 MHz frequency) (Arendash et al., **2010**). The results indicated that long-term EMF exposure led to the suppression of extracellular and intracellular β-amyloid aggregation with the formation of free monomeric forms of β-amyloid that facilitates its removal from brain tissue. Furthermore, Arendash and colleagues repeatedly showed that that long-term EMF treatment can provide general cognitive benefit to very old normal mice, as well as prevent memory impairment (if given in adulthood) and reverse memory impairment (if given in older age) in AD transgenic mice (Arendash et al., **2010**; Arendash et al., **2012**).

In the present study, we investigated some cellular responses to mobile phone frequency EMF in the presence of $A\beta_{42}$ oligomers and H_2O_2. In particular, we exposed human and rat primary astrocytes to EMF of 918 MHz frequency to elucidate its ability to suppress ROS generation via NADP-oxidase and mitochondria and phosphorylation of p38MAPK and ERK1/2. Our choice of the cells was dictated by the latest research data on the role of astrocytes in the progression of AD (Iram and Frenkel, **2012**; Kraft et al., **2013**; Phillips et al., **2014**; Hol, **2015**; González-Reyes et al., **2017**). A number of studies have demonstrated that astrocyte functions change in AD brains. In vitro and in vivo experiments confirmed that $A\beta_{42}$ induces oxidative stress, alters mitochondria and calcium homeostasis, disrupts gliotransmission and triggers cell signaling pathways leading to the production of pro-inflammatory cytokines and chemokines in astrocytes. Moreover, there is data indicating that changes in astrocytes precede neuronal dysfunctions in AD, which points out an important role of astroglia in the progression of the disease.

EXPERIMENTAL PROCEDURES

Cell culture

All procedures related to isolation of human and rat primary astrocytes were performed according to the protocols approved by the Ethics Committee of the Center for Life Sciences of Nazarbayev University (Registration number IORG 0006963). Fetal brains were obtained from the National Scientific Medical Centre (Astana, Kazakhstan). Written informed consent was signed by all patients prior to the experiments.

Primary rat astrocytes were isolated from sixteen one-day-old neonatal Wistar rats according to the protocol described previously (Allen et al., **2000**). Briefly, brains were isolated from anesthetized pups, then cortices were dissected and triturated. Cells were dissociated in a medium containing S-MEM and 3 U/ml dispase. After 10 min of incubation cells were rinsed, centrifuged and resuspended in complete astrocytes growth medium and plated at a concentration of 10,000 viable cells/ml. After 2.5 weeks the purity of culture was assessed using immunofluorescence labeling of GFAP marker.

Primary human astrocytes were isolated from three 17-week old human fetal brains (cerebral cortex) according to previously described protocol with minor modifications (Sharif and Prevot, **2012**). Briefly, the brains were dissected, triturated and trypsinized in 0.25% trypsin at 37 °C for 15 min. Cell suspension was filtered through 100 μm mesh (Falcon), centrifuged and resuspended in complete astrocyte medium (DMEM supplemented with 10% FBS and 1% penicillin/streptomycin). Cells were seeded into T75 cell culture flask in concentrations 1×10^6 cells/ml and incubated at 37 °C with 5% CO_2 to yield for viable and healthy cells. Further, for purification purposes the flask was put on a shaker for two hours at 240 rpm followed by removal of the medium containing glial suspension. Attached cells were cultivated to 90% confluence, stained for astrocyte marker GFAP to confirm their astrocyte nature.

Preparation of $A\beta_{42}$ oligomers

Protocol proposed by Dahlgren et al. was used for the preparation of oligomeric forms of Aβ with modifications (Dahlgren et al., **2002**). Briefly, 1 mg of the $A\beta_{42}$ synthetic peptide (AnaSpec) was suspended in 200 μl of 100% 1,1,1,3,3,3 hexafluoro-2-propanol (HFIP) and aliquoted into 1.5 ml centrifuge tubes. HFIP was removed by evaporation in Eppendorf Concentrator Plus with the integrated vacuum pump, $A\beta_{42}$ was diluted in 2 μl DMSO to phenol free 100 μM in ice-cold culture Ham's medium, sonicated for 60 s, and incubated at 37 °C for 2 h. The presence of the oligomeric form of $A\beta_{42}$ was verified by Western blot analysis (Fig. 1).

EMF exposure set-up and cell treatment

Astrocytes were serum starved for 4 h by replacing DMEM containing 10% FBS with serum-free DMEM followed by exposure to 5 μM of $A\beta_{42}$ oligomers, 0.5 mM of H_2O_2 (Sigma Aldrich) or 2.5 μM of staurosporine (Sigma Aldrich) for 60 min in EMF. Both cell morphology and MTT assay showed that EMF of 918 MHz irradiation did not cause any ill-effect to cell viability up to 24 h. of exposure (data not shown). The unexposed cells were used as controls.

The experimental set-up consisted of signal generators, antennas, an EMF spectrum analyzer, and a Faraday cage.

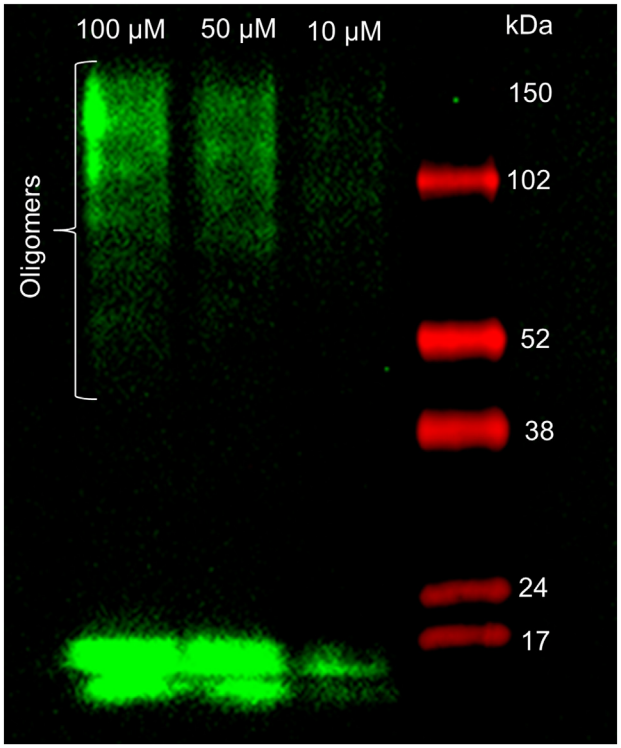


Fig. 1. Western blot: assessment of $A\beta_{42}$ under oligomer-forming conditions.

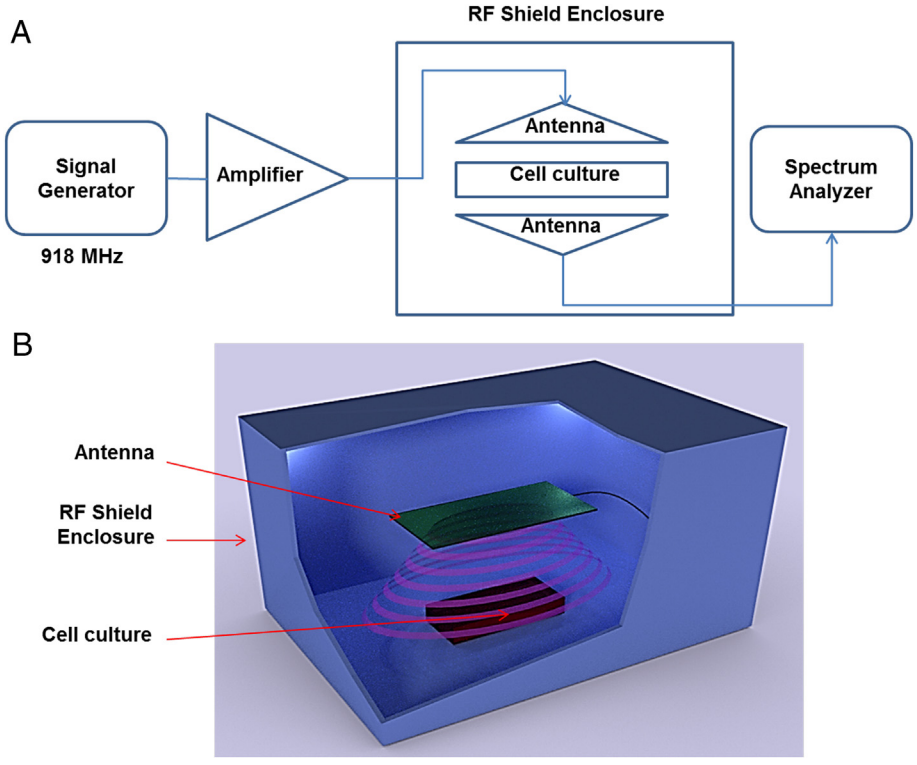


Fig. 2. Principle electric line scheme of exposure of cell culture to electromagnetic field inside RF Shield Exposure Cage (A). 3D scheme of irradiation of cell culture to electromagnetic field inside RF Shield Exposure Cage (Faraday Cage) (B).

As a portable Faraday cage, RF Shielded Test Enclosure, PTC-JRE 0814, Rainford EMC Systems Ltd. (UK), was employed for the experiments (Fig. 2). This system provides full protection from external EMFs, and it allows exposing the cell culture to electromagnetic signals with frequencies up to 6 GHz.

The Faraday cage with astrocytes culture was placed into an incubator (37 °C; 5% CO_2). The electromagnetic exposure was carried out by using an internal radiating antenna mounted above astrocytes culture plate on the distance of 6 cm from the plate (far-field region). This distance is the place, where the far-field region begins and Fresnel zone ends. It was calculated using the following formula (1):

$$Far\ Field\ Region = \frac{2\,(D)^2}{\lambda} \quad (1)$$

where D is the largest dimension of the antenna and λ is the wavelength of 918 MHz frequency.

Such a distance allows avoiding disordered near-field energy distribution, multiple interfering reflections and provides a homogeneous EMF field (Zhao, **2005**). The radiating antenna was connected to a portable source signal USB-compatible generator (Lab Brick LMS series, USA). The culture was exposed to EMF with a frequency of 918 MHz at 10 W peak power pulsed amplitude modulation with a pulse width of 0.580 ms and a repetition rate of 217 Hz.

The specific absorption rate (SAR) (W/kg) can be defined as the ratio of the absorbed power per unit mass of cells / tissue, and it can be expressed as follows (2):

$$SAR = \frac{\sigma |E|^2}{\rho} \quad (2)$$

Here, E is the peak value of the electric field, p is the given mass density of cells (kg/m^3) and σ is the conductivity of cell culture (monolayer) (McIntosh et al., **2003**). In our experiments, the average SAR at the bottom of the medium was 0.20 W/kg.

To determine the impact of thermal effects caused by EMF, a special calibrated fiber optic sensor TS3 thermocouple (OPTOCON, Germany) was utilized for temperature monitoring. TS3 thermocouple provides a stable temperature measurement at EMF/RF environment. “FOTEMP-Assistant” software (OPTOCON, Germany) running on Microsoft Windows operating system was used for temperature monitoring and analysis. The results of thermal monitoring showed no significant rise of temperature as a result of the EM exposure (Fig. 3).

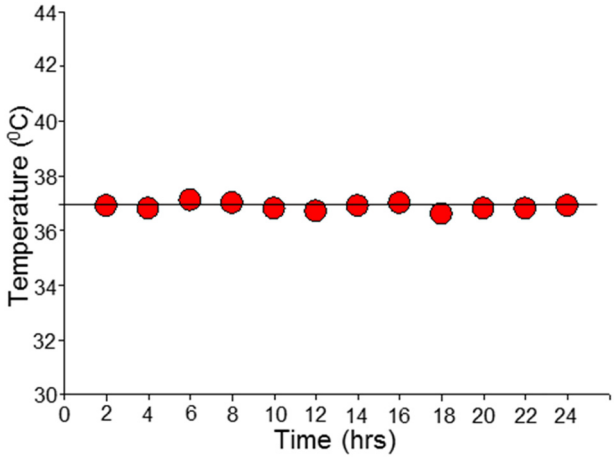


Fig. 3. The results of temperature measurements of cell culture exposed to RF-EM radiation (inside Faraday Cage).

Determination of general ROS

General ROS produced in astrocytes were measured using cell permeable chloromethyl derivative of 2′,7′-dichlorodihydrofluorescein diacetate (CM-H2DCFDA) (Life Technologies). For ROS measurements, cells were seeded in 96 well plates, starved for 4 h and then treated with $A\beta_{42}$ and H_2O_2 in phenol-red free DMEM followed by exposure to EMF. According to manufacturer protocol cells were incubated with CM-H2DCFDA (2.5 μM) for 60 min. Fluorescent intensity of CM-H2DCFDA were measured using microplate reader Synergy H1 and normalized to control.

Determination of mitochondrial ROS

For fluorescent imaging of astrocytes labeled with MitoSox cells were seeded on round (20 mm) coverslips. The next day after starvation and treatment procedures mitochondrial superoxide indicator MitoSOX (5 μM) was added to the cells for 10 min at 37 °C according to the manufacturer's protocol. Cells were then washed and counterstained with DAPI. After washing in PBS cells were mounted in the buffer and observed under fluorescent microscope Carl Zeiss Observer Z1.

For the quantitative assessment of superoxide production in mitochondria, cells were seeded on 96 well plates and cultured overnight. The next day after starvation and treatment procedures MitoSOX reagent was applied to each well under the same conditions as in the fluorescent microscopy experiment described above, and then cells were washed in PBS. Fluorescent intensity of MitoSOX was measured using microplate reader Synergy H1 and normalized to control.

Mitochondrial membrane potential measurement

Mitochondria membrane potential assay kit (USA, Sigma Aldrich) was used to measure mitochondria membrane potential (MMP) in astrocytes. The kit protocol is based on cells staining by lipophilic fluorescent dye JC-10. In mitochondria with polarized membranes JC-10 is retained in the form of aggregates with emission in red spectra, while in the cells with disrupted MMP the dye reverses to the monomeric form with emission in green spectra. The ratio of red/green fluorescent intensity is used to determine MMP. According to the manufacturer protocol cells were plated overnight in 96 well black plates with the clear flat bottom. Before treatment cells were starved for 4 h. in serum-free medium. After treatment 50 μl of the JC-10 dye loading solutions were added to each sample well for 30 min., followed by 50 μl assay buffer loading to the wells. Fluorescent intensity of stained cells was measured at 490/525 nm and 540/590 nm of excitation and emission wavelengths in a microplate reader Synergy H1. The ratio between red and green fluorescent signal was used to analyze MMP in the cells.

Studies of activation of NADP oxidase

The activation of NADPH-oxidase results in translocation of its cytosolic subunit (e.g. p47phox) to the cell membrane and membrane-associated subunits such as gp91phox (DeLeo et al., **1999**; Samuelson et al., **2001**). We used confocal microscopy to quantify co-localization of gp91phox and p47phox on the surface of the astrocytes. The protocol was previously described by Yang et al. (**2010**). Briefly, after the treatments cells were fixed with 4% paraformaldehyde at 37 °C for 30 min., PBS containing 5% BSA was then applied to cells for 1 h. to block nonspecific bindings. To label gp91phox at the cell surface, goat polyclonal anti-gp91phox (Santa Cruz Biotechnology, 1:200 dilution) was added and incubated at 4 °C without permeabilization. To label p47phox, cells were then permeabilized with 0.1% Triton X-100 in PBS for 5 min. Rabbit polyclonal anti-p47phox (Santa Cruz Biotechnology, 1:200 dilution) in PBS with 1% BSA was then added and incubated at 4 °C overnight. This was followed by fluorescent labeling with secondary antibodies (1:500 dilution) at room temperature for 1 h. The secondary antibodies for gp91phox and p47phox were Alexa 488 donkey anti-goat antibody (Life Technologies), and Alexa 594 chicken anti-rabbit antibody (Life Technologies), respectively. Secondary antibodies did not show immunostaining in the absence of the primary antibody (data not shown). Confocal immunofluorescence microscopy was performed with Carl Zeiss LSM700 confocal microscope. Confocal images were acquired with a 60X, numerical aperture 1.2 oil immersion objective lens for co-localization studies between NADPH oxidase subunits, gp91phox and p47phox. To determine the spatial co-localization of labeled objects Z-stack series at 1 μm spacing were captured. Background subtraction was done for all images before analysis. The colocalization indexes between two channels were calculated by normalizing the coincident intensity (yellow) to the total intensity of the corresponding channel as described previously (Askarova et al., **2011**).

MAP kinases assay

The total concentration and the phospho-kinase/total kinase ratio for the p38 MAPK and ERK1/2 were measured in a whole cell lysate using MSD MAP Kinase Total and Phosphoprotein Assay Kits (Meso Scale Discovery). All procedures were performed according to the manufacturer's protocol. Briefly, whole cell lysate was prepared using buffer provided with the kit. Cellular debris was cleared from the

lysate by centrifugation at 10000 x g for 10 min. To make the sandwich for electrochemiluminescence immunoassay, cell lysates were added to the wells of plates pre-coated with capture antibodies and incubated for 3 h. Afterwards the plates were washed 3 times followed by incubation with detection antibody for 1 h. After a final wash, 150 µl of Read Buffer was added to each well and the plates analyzed on MSD QuickPlex SQ 120. Bicinchoninic Acid Assay was used as loading control. Phospho-kinase/total kinase ratios in experimental groups were normalized to untreated control.

Statistical analysis

All the presented data have passed the Shapiro–Wilk test for normality and test for homogeneity of variances, and are expressed as mean ± SEM. A one-way Analysis of Variance (ANOVA) was used to investigate the effects of EMF on ROS formation, MMP, activity of NADPH-oxidase and phosphorylation of p38MAPK and ERK 1/2 kinase in human and rat primary astrocytes in the presence of $A\beta_{42}$ and H_2O_2. When the one-way ANOVA was significant, a post hoc test using the Tukey's pairwise comparison of means was used to reveal differences between various groups. Values were considered significantly different at the $P \leq .05$ level. Statistical analyses were performed on the Stata 13 and SigmaPlot 11.0 software was used to graphically demonstrate the results.

RESULTS

Effect of $A\beta_{42}$, H_2O_2 and EMF on the formation of cellular ROS in human and rat primary astrocytes

To quantify cellular ROS production in astrocytes we utilized the cell permeable chloromethyl derivative of 2′,7′-dichlorodihydrofluorescein diacetate (CM-H2DCFDA), a chemically reduced form of fluorescein dye commonly used as an indicator for ROS in cells. Post hoc comparisons using the Tukey's test followed by ANOVA indicates that 5 µM of $A\beta_{42}$ increases CM-H2DCFDA fluorescence by 51% (M = 1.51, SEM = 0.032) as compared with untreated control (M = 1, SEM = 0.01) in rat primary astrocytes and by 19% (M = 1.19, SEM = 0.012) vs control (M = 1, SEM = 0.012) in human cells, that conforms to data of previously published reports (Cenini et al., **2010**; Schilling and Eder, **2011**). Since H_2O_2 is a known source of ROS, results from the treatment with H_2O_2 served as a positive control. Our data demonstrate 3 to 4 fold increase of ROS formation in both cell types upon hydrogen peroxide exposure (M = 3.01, SEM = 0.046 for rat astrocytes; M = 4.11, SEM = 0.089 for human astrocytes). At the same time, $A\beta_{42}$-stimulated ROS production was attenuated by EMF exposure by 28% in rat astrocytes (M = 1.23, SEM = 0.011) and by 10% in human astrocytes (M = 0.93, SEM = 0.013). Similarly, EMF exposure reduced ROS from H_2O_2 by 70% in rat astrocytes (M = 2.31, SEM = 0.033) and by 140% in human astrocytes (M = 2.58, SEM = 0.053). Moreover, the EMF itself was capable of reducing amount of ROS generated by 27% in human cells (M = 0.73, SEM = 0.012) and by 20% in rat cells (M = 0.8, SEM = 0.008) in comparison with the controls (Fig. 4).

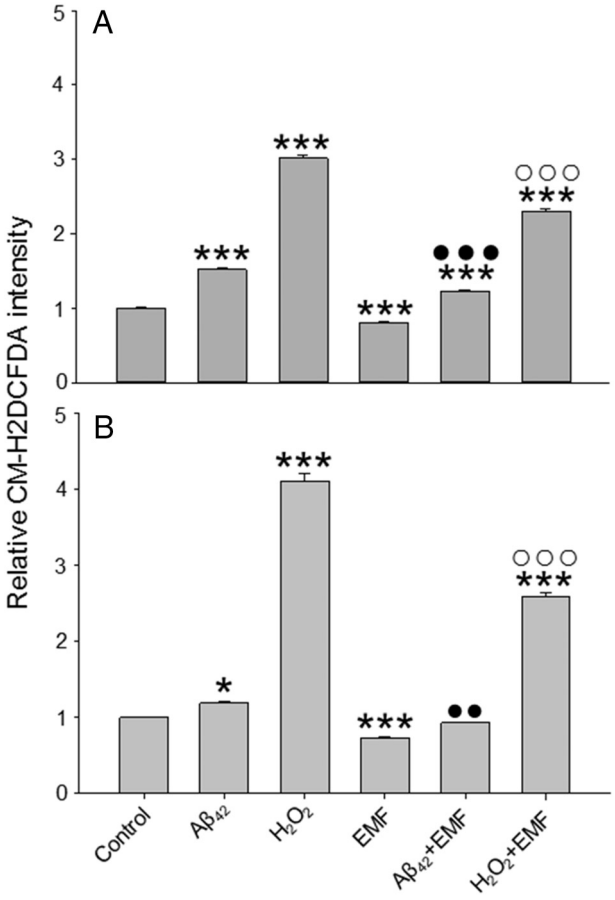


Fig. 4. EMF exposure reduced ROS from $A\beta_{42}$ and H_2O_2 in rat (A) and human (B) primary astrocytes. Level of ROS is represented by relative DCF intensity normalized to the control group. ***$P \leq .001$, *$P \leq .05$ compared to the control; •••$P \leq .001$, ••$P \leq .01$ compared to the group treated with $A\beta_{42}$; ○○○$P \leq .001$ compared to the group treated with H_2O_2 (rat: one-way ANOVA, F(5,42) = 926.46, $P \leq .001$; human: one-way ANOVA, F(5.41) = 895.25, $P \leq .001$).

Effect of $A\beta_{42}$, H_2O_2 and EMF on the formation of mitochondrial ROS in human and rat primary astrocytes

We employed a highly specific mitochondrial superoxide indicator MitoSox to quantify ROS production from mitochondria. As shown on the fluorescent images (Fig. 5A), treatment with $A\beta_{42}$, resulted in increasing of MitoSox intensity in astrocytes. On the contrary, the lower levels of fluorescence were observed in the cells treated with $A\beta_{42}$ in EMF compared to the cells treated solely with $A\beta_{42}$. To confirm visual observations quantitative analysis of fluorescent intensity was performed (Fig. 5B, C). Post hoc comparisons using the Tukey's test indicated that $A\beta_{42}$ treatment resulted in 29% increase of mitochondrial ROS in rat astrocytes (M = 1.29, SEM = 0.06) and in 12% increase in human cells (M = 1.11, SEM = 0.016) compared to untreated controls (M = 1, SEM = 0.054; and M = 1, SEM = 0.016; for rat and human astrocytes respectively), whereas, H_2O_2 did not significantly affect mitochondrial ROS in both cell types. In turn, $A\beta_{42}$ mediated mitochondrial ROS was suppressed by the exposure to EMF by 38% in rat astrocytes (M = 0.92, SEM =

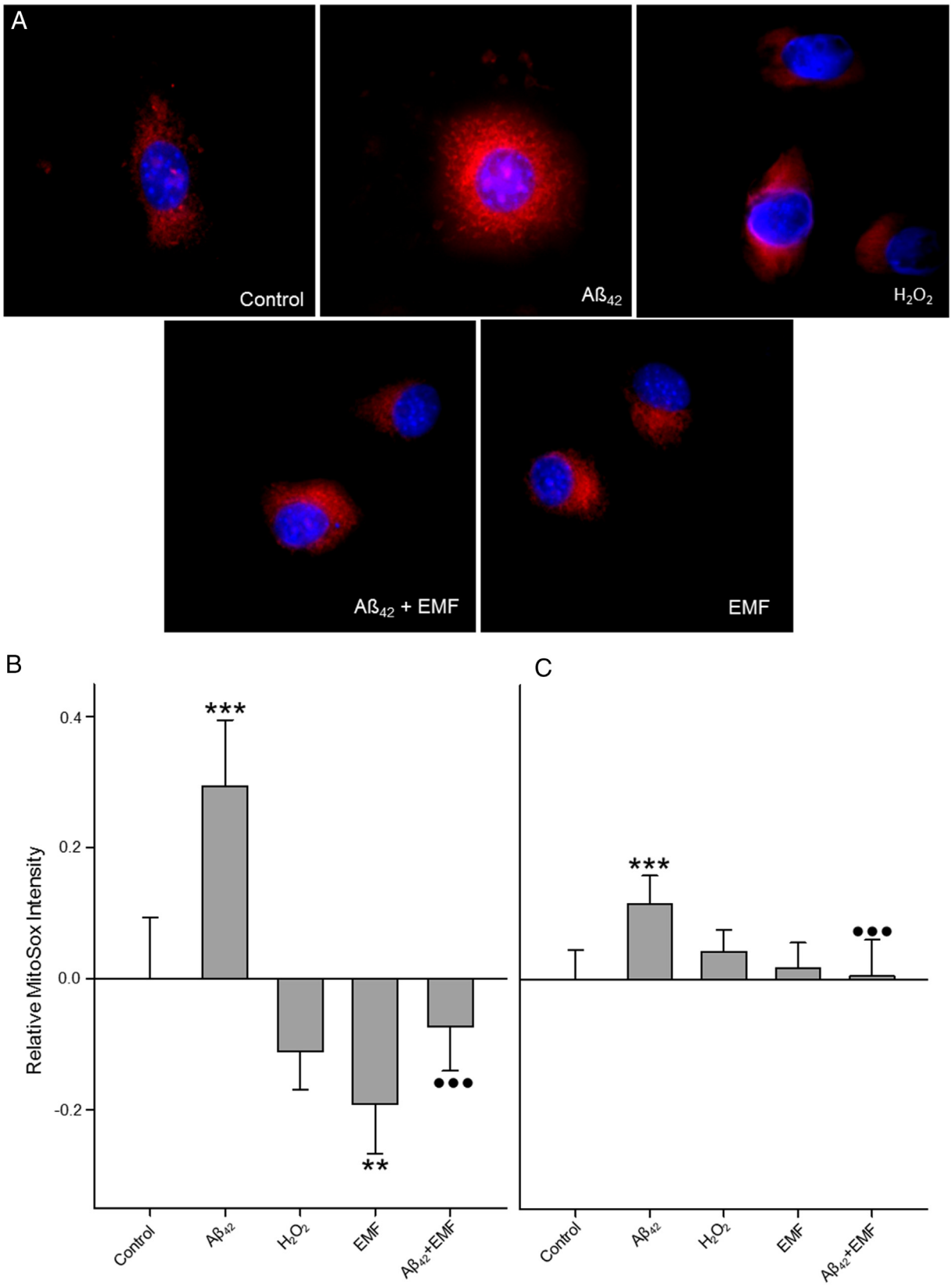


Fig. 5. EMF decreased mitochondrial ROS formation induced by $A\beta_{42}$ in rat and human primary astrocytes. Fluorescent images of rat primary astrocytes labeled with MitoSox (A), quantitative analysis of mitochondrial ROS in rat (B) and human (C) primary astrocytes. Quantitative data represents fluorescent intensity of MitoSox normalized to the control group (zero base line). ***$P \leq .001$, **$P \leq .01$, compared to the control; •••$P \leq .001$ compared to the group treated with $A\beta_{42}$ (rat: one-way ANOVA, $F(5, 130) = 12.08$, $P \leq .001$; human: one-way ANOVA, $F(4, 31) = 8.46$, $P \leq .001$).

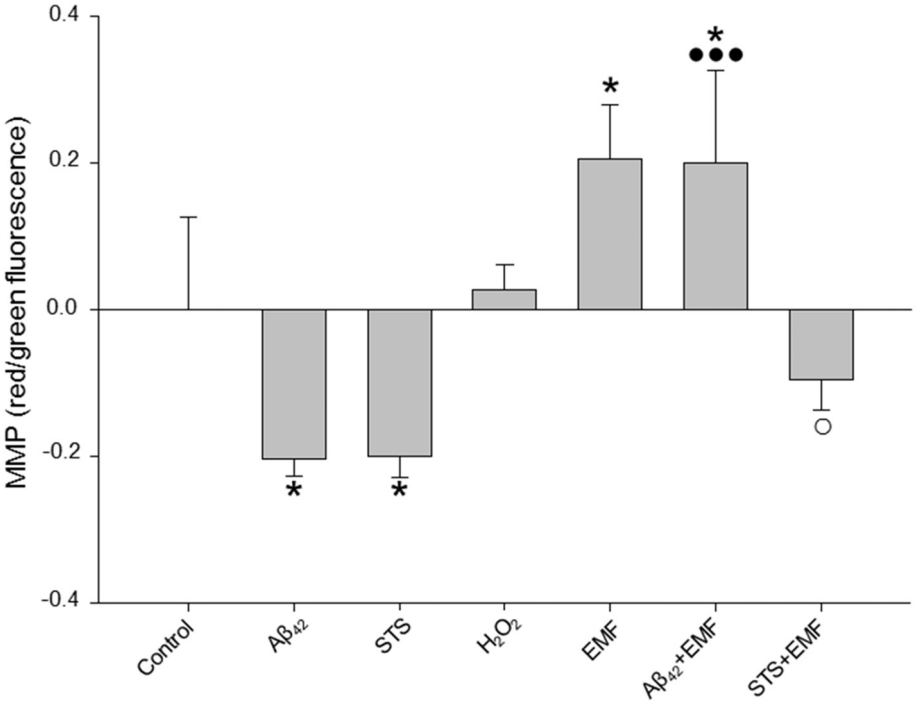


Fig. 6. EMF increases mitochondrial membrane potential in rat primary astrocytes. Quantitative data represents fluorescent intensity of cells labeled with JC10 and normalized to the control group (zero base line). $^{*}P \leq .05$, compared to the control; $^{\bullet\bullet\bullet}P \leq .001$ compared to the group treated with $A\beta_{42}$; $^{\circ}P \leq .05$ compared to the group treated with STS (one-way ANOVA, $F(6, 76) = 6.47$, $P \leq .001$).

0.04) and by 11% in human astrocytes (M = 1, SEM = 0.02). Furthermore, in rat primary astrocytes the application of EMF alone reduced the amount of superoxide anion generated in mitochondria by 20% (M = 0.8, SEM = 0.046) as compared to unexposed cells.

Effect of $A\beta_{42}$, H_2O_2 and EMF on the mitochondrial membrane potential in rat primary astrocytes

There is evidence supported by number of experimental models that ROS production in mitochondria strongly correlates with mitochondrial membrane potential (MMP) (Turrens, **2003**; Esteras Gallego et al., **2015**). Here we investigated the effects of $A\beta_{42}$, H_2O_2 and EMF on RF-MMP in rat primary astrocytes. In agreement with previous reports (Sarkar et al., **2014**) Fig. 6 shows that 5 μM of $A\beta_{42}$ lowers MMP by 20% (M = 0.79, SEM = 0.019) compared to untreated astrocytes (M = 1, SEM = 0.091). Similar results were seen upon treatment with 2.5 μM of staurosporine (STS) (M = 0.8, SEM = 0.023). STS is a well-known inhibitor of protein kinases which induces mitochondria membrane depolarization (Scarlett et al., **2000**). In our experiments STS treatment served as a positive control. In contrast, H_2O_2 treatment did not result in significant MMP change. At the same time, $A\beta_{42}$- and STS-stimulated mitochondrial membrane depolarization was reversed by EMF exposure (40% increase compared to $A\beta_{42}$ alone, M = 1.2, SEM = 0.053; 10% compared to STS alone, M = 0.9, SEM = 0.032). Moreover, EMF itself was capable of increasing mitochondrial membrane potential by 20% in rat primary astrocytes (M = 1.2, SEM = 0.053) compared to untreated cells, which is consistent with MitoSox quantification results showing that EMF decreased the amount of ROS in mitochondria (Fig. 5).

Effect of $A\beta_{42}$ and EMF on NADPH-oxidase activation in rat primary astrocytes

NADPH-oxidase is an enzyme complex consisting of gp91-phox, p22-phox membrane-bound subunits, three cytosolic subunits (p67-phox, p47-phox and p40-phox), and a low-molecular-weight G protein (Babior, **1999**). It has been shown that NADPH-oxidase contributes actively to the production of ROS in astrocytes (Qing et al., **2005**; Zhu et al., **2009**; Sheng et al., **2013**). Since activation of this kinase is associated with the migration of the cytosolic components to the cell membrane and assembling with its membrane subunits, we tested the effects of $A\beta_{42}$ and EMF on co-localization of gp91phox and p47phox subunits by analyzing confocal images of double immunofluorescent-labeled gp91-phox and p47-phox in rat primary astrocytes (Fig. 7A).

Post hoc comparisons using the Tukey's test indicated that $A\beta_{42}$ significantly increased assembling of cytosolic subunit p47-phox of NADPH-oxidase with its membrane subunits gp91-phox (by 28%) suggesting $A\beta_{42}$ induced NADPH-oxidase activation (M = 1, SEM = 0.09 for control group and M = 1.28, SEM = 0.07 for $A\beta_{42}$ group). In turn, exposure of astrocytes to EMF of 918 MHz frequency suppressed the co-localization of p47-phox with gp91-phox induced by $A\beta_{42}$ (by 31%, M = 0.97, SEM = 0.06). Our data also showed that EMF itself did not significantly reduce activity of the NADPH-oxidase. To verify this method of measurement for NADPH-oxidase activity, we demonstrated that NADPH-oxidase inhibitor (gp91 ds-tat) suppressed Aβ-mediated increase in co-localization of gp91phox and p47phox (Fig. 7B).

Effect of $A\beta_{42}$, H_2O_2 and EMF on phosphorylation of p38MAPK and ERK1/2

Mitogen-activated protein kinases (MAPKs) are serine/threonine protein kinases that regulate the signaling of many extracellular stimuli from the plasma membrane to the nucleus. There is evidence suggesting the involvement of MAPK/ERK downstream signaling pathways in cellular responses induced by oxidative stress and $A\beta_{42}$ (Askarova et al., **2011**; Emmanuelle et al., **1997**; Xu et al., **2001**; Yin et al., **2002**; Hsu et al., **2007**; Shelat et al., **2008a**). Here, we tested whether irradiation of rat primary astrocytes with EMF of

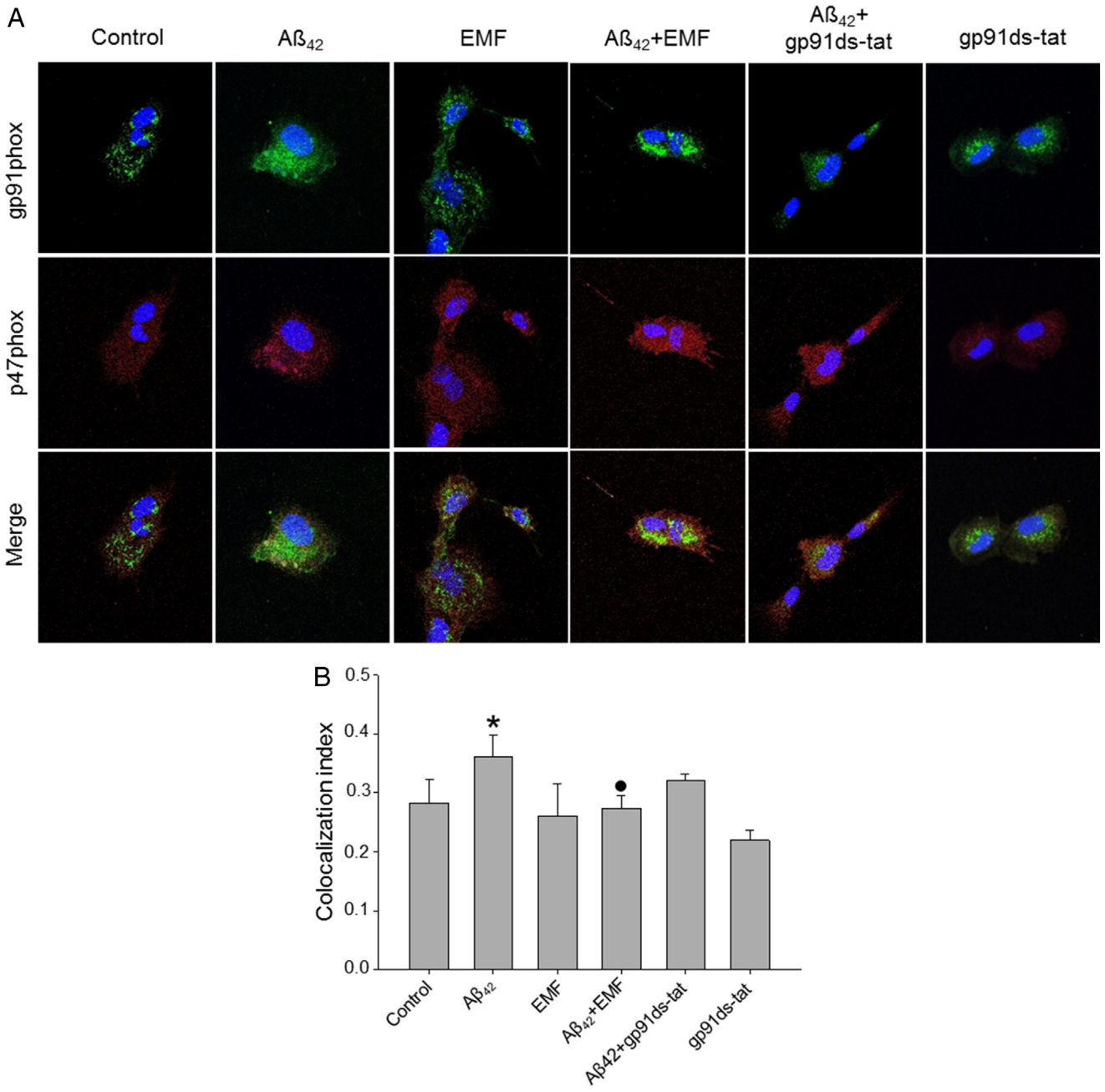


Fig. 7. EMF suppresses induced by $A\beta_{42}$ activation of NADPH-oxidase in rat primary astrocytes. NADPH-oxidase activity is represented by coefficient of gp91phox and p47phox subunits co-localization (normalized to the control group). Confocal images (A), quantitative analysis (B). ***P** ≤ .05 compared to the control; **•P** ≤ .05 compared to the group treated with $A\beta_{42}$ (one-way ANOVA, $F(5,70) = 2.71$, ***P*** ≤ .05).

918 MHz frequency is capable of modulating the activity p38MAPK and ERK1/2.

In agreement with the previous reports, results obtained from Meso Scale Discovery immunoassay (Fig. 8) showed that $A\beta_{42}$ exposure lead to increase of phosphorylation of p38MAPK by 103% (M = 2.03, SEM = 0.38) and ERK1/2 by 24% (M = 1.24, SEM = 0.065) as compared to untreated controls (M = 1, SEM = 0.067 for p38MAPK and M = 0.99, SEM = 0.031 for ERK1/2). Similarly, Post hoc comparisons using the Tukey's test indicated that treatment with H_2O_2 resulted in a 54% increase in Phospho/Totalp38MAPK ratio (M = 1.54, SEM = 0.054) and a 32% increase in Phospho/TotalERK1/2 ratio (M = 1.32, SEM = 0.038). Our data also demonstrated that pre-treatment of astrocytes with EMF alone did not change phosphorylation of MAPKs and did not suppress $A\beta_{42}$-induced phosphorylation of the kinases. However, EMF significantly decreased H_2O_2-induced phosphorylation of p38MAPK (by 50%) and ERK1/2 (by 12%) (M = 1.02, SEM = 0.06 and M = 1.2, SEM = 0.016 respectively). Since the activation of these kinases

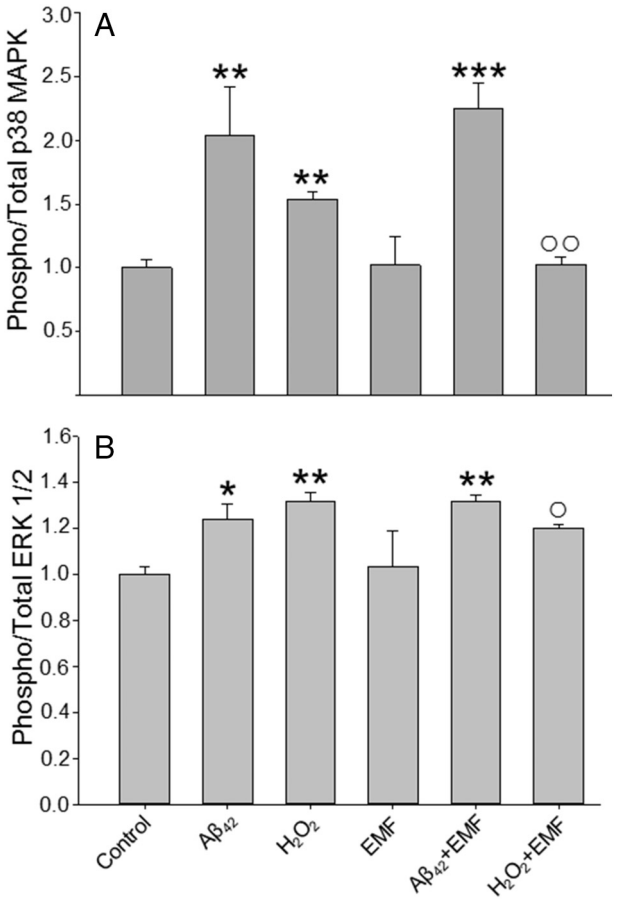


Fig. 8. EMF suppresses H_2O_2 –induced phosphorylation of p38MAPK (A) and ERK1/2 (B), but does not attenuate $A\beta_{42}$-induced activation of the MAPKs in rat primary astrocytes. ***$P \leq .001$, **$P \leq .01$, *$P \leq .05$ compared to the control; $^{OO}P \leq .01$, $^{O}P \leq .05$ compared to the group treated with H_2O_2 ((A)one-way ANOVA, F(5, 12) = 7.3, $P \leq .01$; (B) – one-way ANOVA, F(5, 12) = 3.55, $P \leq .05$).

happens via phosphorylation, this implies changes in their activity.

DISCUSSION

Amyloid beta peptide has been reported to mediate oxidative damage in astrocytes and trigger the downstream mitogen-activated protein kinase/extracellular signal-regulated kinase (MAPK/ERK) pathway (Askarova et al., **2011**; Serrano et al., **2009**; Schilling and Eder, **2011**; Gao et al., **2012**; Swomley and Butterfield, **2015**). The present study demonstrated that the exposure of astrocytes to EMF with a frequency of 918 MHz increased mitochondrial membrane potential, suppressed $A\beta_{42}$-induced ROS production from NADPH-oxidase and mitochondria, inhibited H_2O_2–induced phosphorylation of p38MAPK and ERK1/2, and may potentially be used for the protection of brain cells against β-amyloid induced oxidative stress.

A frequency of 918 MHz corresponds to the electromagnetic range that is widely used in conventional mobile phones. Data of our experiments are consistent with the results of the study of Arendash et al. (**2010**), Arendash et al. (**2012**). In these studies, transgenic mice with AD were exposed to EMF with the frequency of 918 MHz (GSM, pulsed/modulated signal) during 6 months. The electromagnetic irradiation resulted in the suppression of β-amyloid deposition in brain cells and improved cognitive function of mice affected by AD. In our study, we used the same EMF parameters (918 MHz), but we employed human and rat primary astrocytes and shorter period of irradiation (60 min.) to reveal cellular responses to mobile phone frequency EMF in the presence of $A\beta_{42}$ and H_2O_2.

In another work conducted by the same research group a long-term exposure of animals to high frequency EMF (918 MHz frequency) led to an increase of brain mitochondrial function in Alzheimer's transgenic mice, and the EMF-induced enhancement of brain mitochondrial function was accompanied by increases in soluble Aβ (Dragicevic et al., **2011**). The authors hypothesized that the observed increase of mitochondrial soluble β-amyloid peptide was caused by the ability of EMF to disaggregate Aβ-oligomers. It was also demonstrated that EMF-induced mitochondrial enhancement occurred through non-thermal effects because brain temperatures were either stable or decreased during/after EMF treatment.

Mitochondria are considered as the main site for ROS generation, and there is a number of reports on Aβ-induced mitochondrial dysfunction and oxidative stress in astrocytes (Abramov et al., **2004**; Abramov and Duchen, **2005**; Zhu et al., **2006**). In turn, the ROS in mitochondria originate from mitochondrial respiratory chain due to a leak of electrons and their reactions with oxygen molecules, and amount of generated ROS strongly correlates with MMP (Turrens, **2003**; Esteras Gallego et al., **2015**). It is generally believed that more ROS is produced by mitochondria if MMP increases (Esteras Gallego et al., **2015**)(Miwa and Brand, **2003**). However, there is data demonstrating that some pathological conditions associated with the dysfunctions of the respiratory chain components or presence of $A\beta_{42}$ oligomers cause a reduction in mitochondrial membrane potential and a simultaneous increase in ROS production (Lebiedzinska et al., **2010**; Sarkar et al., **2014**; Song et al., **2017**). In agreement with this concept, we observed that $A\beta_{42}$ increased the amount of ROS in mitochondria and decreased mitochondrial membrane potential. However, RF-EMF could attenuate $A\beta_{42}$-induced mitochondrial membrane depolarization and elevation of mitochondrial ROS. Moreover, RF-EMF alone caused the reduction of the amount of superoxide anion generated in mitochondria which was accompanied by the significant increase in MMP.

MMP collapse coincides with the opening of the mitochondrial permeability transition pore (MPTP)(Ly et al., **2003**). In turn, Aβ has been shown to augment mitochondrial membrane potential either indirectly by promoting the expression of proteins associated with the MPTP or by directly binding to the membranes and forming ion-permeable pores (Kandel et al., **2017**). The observed increase in the MMP upon exposure to EMF may be explained by downregulation of MPTP formation or inhibition of ATP synthase, while suppression of ROS generation happens due to reduction of electron transport. Thus, our finding suggests a direct effect

of the electromagnetic field on membrane biophysical properties that may lead to restoration of mitochondrial functions affected by β-amyloid. Since we did not detect any significant temperature elevation during EM exposure, the observed impact of EMF on molecular processes can be attributed to non-thermal effects.

Plasma membrane-bound enzyme complex NADPH-oxidase is another source of superoxide anions induced by Aβ in astrocytes and neurons (Qing et al., **2005**; Shelat et al., **2008b**; Brennan et al., **2009**; Zhu et al., **2009**). Moreover, there are data indicating that β-amyloid induces mitochondrial dysfunction through activation of NADPH-oxidase (Abramov et al., **2004**), and it is considered as the primary source of astrocytic superoxide induced by Aβ (Abramov and Duchen, **2005**). In agreement with this concept, our results demonstrated that $A\beta_{42}$ induced NADPH-oxidase activation, while EMF exposure resulted in suppression of $A\beta_{42}$-mediated increase in co-localization of gp91phox and p47phox. It has been reported that EMF exposure results in changes in membrane potential, modification of membrane proteins and modulation of activity of ion channels (Ross et al., **2015**; Krutáková et al., **2016**). In our study RF-EMF induced a significant increase in MMP. We suggest that EMF is able to modulate the electrical potentials on the plasma membranes as well, thus affecting cell membrane proteins. This leads to translocation of active molecular complexes including modulation of the activity of NADPH oxidase. As a result, we observed the suppression of ROS production ('treated with β-amyloid' and 'not treated with β-amyloid' groups) in rats and humans astrocytes. Interestingly, the inhibition of cellular ROS formation by means of EMF was also detected in the groups treated solely with peroxide hydrogen.

It is well known that Aβ oligomers and ROS can initiate the downstream mitogen-activated protein kinase/extracellular signal-regulated kinase (MAPK/ERK) pathway (Askarova et al., **2011**; Zhu et al., **2002**; Son et al., **2013**). Five groups of MAPKs have been characterized in mammalian cells: extracellular signal-regulated kinases 1 and 2 (ERK1/2), c-Jun amino-terminal kinases, p38 MAPKs, ERK3/4, and ERK5, and the most extensively studied MAPKs are the ERK1/2 and p38 kinases (Roux and Blenis, **2004**).In the present study, we explored the effects of EMF on the phosphorylation of p38MAPK and ERK1/2 kinases induced by β-amyloid and hydrogen peroxide. We observed the ability of EMF to suppress phosphorylation of p38MAPK and ERK1/2 induced by H_2O_2. Yet, EMF was not able to modulate alterations in the phosphorylation state of the MAPKs triggered by $A\beta_{42}$. Previously, we showed the feasibility of the existence of two independent pathways for kinase phosphorylation activated by $A\beta_{42}$ (Askarova et al., **2011**). One of them is associated with activation of NADPH-oxidase and elevated ROS production in the mouse brain endothelial cells (bEnd3). However, in the primary rat astrocytes RAGE (receptor for advanced glycation end-products) acts as a signal transducing cell surface receptor for $A\beta_{42}$ to trigger phosphorylation of ERK1/2 which does not require activation of NADPH-oxidase and generation of ROS. In our study, the detected inability of EMF to prevent phosphorylation of p38MAPK and ERK1/2 kinases induced by $A\beta_{42}$ can be explained by the second ROS-independent downstream pathway, albeit this is speculation.

In summary, our data showed that EMF treatment of brain cells with parameters similar to irradiation from the ordinary mobile phone (918 MHz; GSM) was capable of suppressing oxidative stress triggered by $A\beta_{42}$ and H_2O_2, thus indicating its possible therapeutic benefit. Our data conform to the previous reports on beneficial impact of EMF that can be employed for the treatment of neurodegenerative disorders such as Alzheimer's disease. However, further studies are needed to validate the effectiveness and safety of EMF application in AD patients.

AUTHOR CONTRIBUTIONS

Conceptualization, Sholpan Askarova and Timur Saliev; Funding acquisition, Sholpan Askarova and Timur Saliev; Investigation, Andrey Tsoy, Elvira Abzhanova, Anel Turgambayeva, Bauyrzhan Umbayev; Methodology, Andrey Tsoy, Timur Saliev, Mars Akishev and Sholpan Askarova; Statistical analysis, Aiym Kaiyrlykyzy; Resources, Samat Saparbayev; Supervision, Sholpan Askarova; Writing – original draft, Andrey Tsoy, Timur Saliev and Sholpan Askarova; Writing – review & editing, Sholpan Askarova.

CONFLICTS OF INTEREST

The authors declare no conflict of interest.

ACKNOWLEDGMENTS

The work was funded through the grants of the Ministry of Education and Science of the Republic of Kazakhstan №№ 0115RK00342 and AP05133266.

REFERENCES

Anon . (2018) Alzheimer's disease facts and figures. Alzheimer's Association annual report.

Abramov AY, Canevari L, Duchen MR. (2004) Beta-amyloid peptides induce mitochondrial dysfunction and oxidative stress in astrocytes and death of neurons through activation of NADPH oxidase. J Neurosci 24:565-575.

Abramov AY, Duchen MR. (2005) The role of an astrocytic NADPH oxidase in the neurotoxicity of amyloid beta peptides. Philos Trans R Soc Lond B Biol Sci 360:2309-2314.

Allen JW, Mutkus LA, Aschner M. (2000) Isolation of neonatal rat cortical astrocytes for primary cultures. Curr. Protoc. Toxicol. 4:12.4.1-12.4.15.

Arendash GW, Mori T, Dorsey M, Gonzalez R, Tajiri N, Borlongan C. (2012) Electromagnetic treatment to old Alzheimer's mice reverses beta-amyloid deposition, modifies cerebral blood flow, and provides selected cognitive benefit. PLoS One 7e35751.

Arendash GW, Sanchez-Ramos J, Mori T, Mamcarz M, Lin XY, Runfeldt M, Wang L, Zhang GX, Sava V, Tan J, Cao C. (2010) Electromagnetic field treatment protects against and reverses cognitive impairment in Alzheimer's disease mice. J Alzheimers Dis 19:191-210.

Askarova S., Yang X., Sheng W., Sun G.Y., Lee J.C.. (2011) Role of Abeta-receptor for advanced glycation endproducts interaction in oxidative stress and cytosolic phospholipase A(2) activation in astrocytes and cerebral endothelial cells. Neuroscience 199:375-385.

Babior BM. (1999) NADPH Oxidase: An Update. Blood 93:1464-1476.

Brennan AM, Suh SW, Won SJ, Narasimhan P, Kauppinen TM, Lee H, Edling Y, Chan PH, Swanson RA. (2009) NADPH oxidase is the

primary source of superoxide induced by NMDA receptor activation. Nat Neurosci 12:857-863.
Cenini G, Cecchi C, Pensalfini A, Bonini SA, Ferrari-Toninelli G, Liguri G, Memo M, Uberti D. (2010) Generation of reactive oxygen species by beta amyloid fibrils and oligomers involves different intra/extracellular pathways. Amino Acids 38:1101-1106.
Cline EN, Bicca MA, Viola KL, Klein WL. (2018) The amyloid-beta oligomer hypothesis: beginning of the third decade. J Alzheimers Dis 64: S567-s610.
Dahlgren KN, Manelli AM, Stine WB, Baker LK, Krafft GA, LaDu MJ. (2002) Oligomeric and fibrillar species of amyloid-beta peptides differentially affect neuronal viability. J Biol Chem 277:32046-32053.
DeLeo FR, Allen LAH, Apicella M, Nauseef WM. (1999) NADPH oxidase activation and assembly during phagocytosis. J Immunol 163:6732-6740.
Dragicevic N, Bradshaw PC, Mamcarz M, Lin X, Wang L, Cao C, Arendash GW. (2011) Long-term electromagnetic field treatment enhances brain mitochondrial function of both Alzheimer's transgenic mice and normal mice: a mechanism for electromagnetic field-induced cognitive benefit? Neuroscience 185:135-149.
Emmanuelle MB, Michal T, Robert JM, Bernhard H. (1997) Amyloid β-peptide induces cell monolayer albumin permeability, impairs glucose transport, and induces apoptosis in vascular endothelial cells. J Neurochem 68:1870-1881.
Esteras Gallego N, Wray S, Preza E, Abramov AY. (2015) Higher mitochondrial membrane potential induces ROS production in the familiar form of frontotemporal dementia with MAPT mutations. Biophys J 108:611a.
Gao HM, Zhou H, Hong JS. (2012) NADPH oxidases: novel therapeutic targets for neurodegenerative diseases. Trends Pharmacol Sci 33:295-303.
González-Reyes RE, Nava-Mesa MO, Vargas-Sánchez K, Ariza-Salamanca D, Mora-Muñoz L. (2017) Involvement of astrocytes in Alzheimer's disease from a **neuroinflammatory** and oxidative stress perspective. Front Mol Neurosci 10.
Hanczyc P, Samoc M, Norden B. (2013) Multiphoton absorption in amyloid protein fibres. Nat Photonics 7:969-972.
Hol E. (2015) Astrocytes in the aging brain and in Alzheimer's disease. Glia 63:E69-E70.
Hsu M.-J., Hsu CY, Chen B.-C., Chen M.-C., Ou G, Lin C.-H.. (2007) Apoptosis signal-regulating kinase 1 in amyloid-beta-peptide-induced cerebral endothelial cell apoptosis. J Neurosci 27:5719-5729.
Iram T, Frenkel D. (2012) Targeting the role of astrocytes in the progression of Alzheimer's disease. Curr Signal Transduct Ther 7:20-27.
Kandel N, Zheng T, Huo Q, Tatulian SA. (2017) Membrane binding and pore formation by a cytotoxic fragment of amyloid β peptide. J Phys Chem B 121:10293-10305.
Kennedy JE. (2005) High-intensity focused ultrasound in the treatment of solid tumours. Nat Rev Cancer 5:321-327.
Kraft AW, Hu XY, Yoon H, Yan P, Xiao QL, Wang Y, Gil SC, Brown J, Wilhelmsson U, Restivo JL, Cirrito JR, Holtzman DM, Kim J, Pekny M, Lee JM. (2013) Attenuating astrocyte activation accelerates plaque pathogenesis in APP/PS1 mice. FASEB J 27:187-198.
Krutáková M, Matáková T, Halašová E, Šarlinová M, Špánik P, Janoušek L. (2016) Analysis of electromagnetic field effect on cell plasma membrane potential. 2016 ELEKTRO. p. 547-550.
Lebiedzinska M, Karkucinska-Wieckowska A, Giorgi C, Karczmarewicz E, Pronicka E, Pinton P, Duszynski J, Pronicki M, Wieckowski MR. (2010) Oxidative stress-dependent p66Shc phosphorylation in skin fibroblasts of children with mitochondrial disorders. Biochim Biophys Acta 1797:952-960.
Leinenga G, Gotz J. (2015) Scanning ultrasound removes amyloid-beta and restores memory in an Alzheimer's disease mouse model. Sci Transl Med 7278ra233.
Li JJ, Gu MF, Luo GY, Liu LZ, Zhang R, Xu GL. (2009) Complications of high intensity focused ultrasound for patients with hepatocellular carcinoma. Technol Cancer Res Treat 8:217-224.
Lukiw WJ. (2012) Amyloid beta (Abeta) peptide modulators and other current treatment strategies for Alzheimer's disease (AD). Expert Opin Emerg Drugs 17:43-60.
Ly J, Grubb D, Lawen A. (2003) The mitochondrial membrane potential (deltapsi(m)) in apoptosis, 2003.
Manthe RL, Foy SP, Krishnamurthy N, Sharma B, Labhasetwar V. (2010) Tumor ablation and nanotechnology. Mol Pharm 7:1880-1898.
McIntosh RL, McKenzie RJ, Iskra S, Carratelli A, Standaert P. (2003) Computation of SAR in cell culture flasks exposed to 900 MHz GSM type signals in a modified TEM cell. Appl Comput Electron :107-113.
Miwa S, Brand MD. (2003) Mitochondrial matrix reactive oxygen species production is very sensitive to mild uncoupling. Biochem Soc Trans 31:1300-1301.
Mohammad RM, Muqbil I, Lowe L, Yedjou C, Hsu H.-Y., Lin L.-T., Siegelin MD, Fimognari C, Kumar NB, Dou QP, Yang H, Samadi AK, Russo GL, Spagnuolo C, Ray SK, Chakrabarti M, Morre JD, Coley HM, Honoki K, Fujii H, Georgakilas AG, Amedei A, Niccolai E, Amin A, Ashraf SS, Helferich WG, Yang X, Boosani CS, Guha G, Bhakta D, Ciriolo MR, Aquilano K, Chen S, Mohammed SI, Keith WN, Bilsland A, Halicka D, Nowsheen S, Azmi AS. (2015) Broad targeting of resistance to apoptosis in cancer. Semin Cancer Biol 35:S78-S103.
Phillips EC, Croft CL, Kurbatskaya K, O'Neill MJ, Hutton ML, Hanger DP, Garwood CJ, Noble W. (2014) Astrocytes and neuroinflammation in Alzheimer's disease. Biochem Soc Trans 42:1321-1325.
Prince M, Ali G.-C., Guerchet M, Prina AM, Albanese E, Wu Y.-T.. (2016) Recent global trends in the prevalence and incidence of dementia, and survival with dementia. Alzheimers Res Ther 8:23.
Qing L, Jiu-Hong K, Rong-Liang Z. (2005) NADPH oxidase produces reactive oxygen species and maintains survival of rat astrocytes. Cell Biochem Funct 23:93-100.
Ross CL, Siriwardane M, Almeida-Porada G, Porada CD, Brink P, Christ GJ, Harrison BS. (2015) The effect of low-frequency electromagnetic field on human bone marrow stem/progenitor cell differentiation. Stem Cell Res 15:96-108.
Roux PP, Blenis J. (2004) ERK and p38 MAPK-activated protein kinases: a family of protein kinases with diverse biological functions. Microbiol Mol Biol Rev 68:320-344.
Samuelson DJ, Powell MB, Lluria-Prevatt M, Romagnolo DF. (2001) Transcriptional activation of the gp91phox NADPH oxidase subunit by TPA in HL-60 cells. J Leukoc Biol 69:161-168.
Sarkar P, Zaja I, Bienengraeber M, Rarick KR, Terashvili M, Canfield S, Falck JR, Harder DR. (2014) Epoxyeicosatrienoic acids pretreatment improves amyloid β-induced mitochondrial dysfunction in cultured rat hippocampal astrocytes. Am J Physiol Heart Circ Physiol 306:H475-H484.
Scarlett JL, Sheard PW, Hughes G, Ledgerwood EC, Ku H.-H., Murphy MP. (2000) Changes in mitochondrial membrane potential during staurosporine-induced apoptosis in Jurkat cells. FEBS Lett 475:267-272.
Schilling T, Eder C. (2011) Amyloid-beta-induced reactive oxygen species production and priming are differentially regulated by ion channels in microglia. J Cell Physiol 226:3295-3302.
Serrano F, Chang A, Hernandez C, Pautler RG, Sweatt JD, Klann E. (2009) NADPH oxidase mediates beta-amyloid peptide-induced activation of ERK in hippocampal organotypic cultures. Mol Brain :2.
Sharif A, Prevot V. (2012) Isolation and culture of human astrocytes. Methods Mol Biol 814:137-151.
Shelat PB, Chalimoniuk M, Wang J.-H., Strosznajder JB, Lee JC, Sun AY, Simonyi A, Sun GY. (2008) Amyloid beta peptide and NMDA induce ROS from NADPH oxidase and AA release from cytosolic phospholipase a₂ in cortical neurons. J Neurochem 106:45-55.
Shelat PB, Chalimoniuk M, Wang JH, Strosznajder JB, Lee JC, Sun AY, Simonyi A, Sun GY. (2008) Amyloid beta peptide and NMDA induce ROS from NADPH oxidase and AA release from cytosolic phospholipase A2 in cortical neurons. J Neurochem 106:45-55.
Sheng WS, Hu S, Feng A, Rock RB. (2013) Reactive oxygen species from human astrocytes induced functional impairment and oxidative damage. Neurochem Res 38:2148-2159.
Son Y, Kim S, Chung HT, Pae HO. (2013) Reactive oxygen species in the activation of MAP kinases. Methods Enzymol 528:27-48.
Song SB, Jang S.-Y., Kang HT, Wei B, Jeoun U.-W., Yoon GS, Hwang ES. (2017) Modulation of mitochondrial membrane potential and ROS generation by nicotinamide in a manner independent of SIRT1 and Mitophagy. Mol Cells 40:503-514.

Swomley AM, Butterfield DA. (2015) Oxidative stress in Alzheimer disease and mild cognitive impairment: evidence from human data provided by redox proteomics. Arch Toxicol 89:1669-1680.

Turrens JF. (2003) Mitochondrial formation of reactive oxygen species. J Physiol 552:335-344.

Xu J, Chen S, Ku G, Ahmed SH, Xu J, Chen H, Hsu CY. (2001) Amyloid beta peptide-induced cerebral endothelial cell death involves mitochondrial dysfunction and caspase activation. J Cereb Blood Flow Metab 21:702-710.

Yang X., Askarova S., Sheng W., Chen J.K., Sun A.Y., Sun G.Y., Yao G., Lee J.C.. (2010) Low energy laser light (632.8 nm) suppresses amyloid-beta peptide-induced oxidative and inflammatory responses in astrocytes. Neuroscience 171:859-868.

Yin KJ, Lee JM, Chen SD, Xu J, Hsu CY. (2002) Amyloid-beta induces Smac release via AP-1/Bim activation in cerebral endothelial cells. J Neurosci 22:9764-9770.

Zhao JX. (2005) Numerical dosimetry for cells under millimetre-wave irradiation using petri dish exposure set-ups. Phys Med Biol 50:3405-3421.

Zhu D, Hu C, Sheng W, Tan KS, Haidekker MA, Sun AY, Sun GY, Lee J. C.-M.. (2009) NAD(P)H oxidase-mediated reactive oxygen species production alters astrocyte membrane molecular order via phospholipase A2. Biochem J 421:201-210.

Zhu D, Lai Y, Shelat PB, Hu C, Sun GY, Lee JC. (2006) Phospholipases A2 mediate amyloid-beta peptide-induced mitochondrial dysfunction. J Neurosci 26:11111-11119.

Zhu X, Lee H.-g., Raina AK, Perry G, Smith MA. (2002) The Role of Mitogen-Activated Protein Kinase Pathways in Alzheimer's Disease, 2002.

(Received 6 November 2018, Accepted 27 March 2019)
(Available online 3 April 2019)